Conference paper

Elena Asabina*, Vladimir Pet'kov, Pavel Mayorov, Dmitriy Lavrenov, Igor Schelokov and Andrey Kovalsky

Synthesis, structure and thermal expansion of the phosphates $M_{0.5+x}M'_xZr_{2-x}(PO_4)_3$ (M, M′–metals in oxidation state +2)

DOI 10.1515/pac-2016-1005

Abstract: The phosphates $M_{0.5+x}M'_xZr_{2-x}(PO_4)_3$ (M–Ca, Mn, Co, Sr, Cd, Ba, Pb; M′–Mg, Mn, Co) were synthesized by sol-gel method with the following thermal treatment of reaction mixtures. X-ray diffraction, IR spectroscopy and electron microprobe analysis showed that the obtained phosphates crystallized in $Sc_2(WO_4)_3$ (SW) and $NaZr_2(PO_4)_3$ (NZP) structural types. Both types of crystal structures are based on a framework comprised of octahedra and tetrahedra, the difference between them is fragments orientation. Thermal expansion of the phosphates was studied in the temperature range 20–800 °C. Some compounds were found to belong to low-expanding materials ($\alpha_{av} \sim 2 \cdot 10^{-6}$ °C^{-1}).

Keywords: metal in oxidation state +2; phosphate; SSC-2016; structure; synthesis; thermal expansion; zirconium.

Introduction

Phosphates $M_nL_2(PO_4)_3$ ($0 \le n \le 4$), with $\{[L_2(PO_4)_3]^{p-}\}_{3\infty}$ frameworks (L is an octahedrally coordinated cation, p is a framework charge) have attracted attention of researchers due to their unique set of properties. Mostly, framework phosphates are characterized as highly resistant to the extreme environmental conditions [1], such as high temperatures, wet or aggressive media and various emissions. The majority of discussed options of practical applications of these substances are connected with their controlled, often low thermal expansion [1, 2]. Low-expanding ceramic materials made of phosphates are widely proposed as solid ionic conductors (NASICON) that may well be exploited in a wide range of temperatures [3], thermal shock resistant ceramics, host matrices for nuclear waste immobilization [4], catalysts or supports [5].

These materials are characterized by flexible crystal structure formed by PO_4 tetrahedra sharing corners with LO_6 octahedra. Many variations in linking between PO_4 and LO_6 fragments lead to formation of varied interstitial sites that are intrinsic features of certain structural types [6], such as well-known types of $NaZr_2(PO_4)_3$ (NZP/NASICON, mineral analog is kosnarite $KZr_2(PO_4)_3$, sp. gr. $R\bar{3}c$) and $Sc_2(WO_4)_3$ (SW, sp. gr. $P2_1/n$) [7, 8] (Fig. 1). Two types of framework cavity sites are inherent for NZP structure, being M1, surrounded by six nearest O atoms, and M2, surrounded by eight nearest O atoms (Fig. 1a). When it comes to SW structure,

Article note: A collection of invited papers based on presentations at the 12th Conference on Solid State Chemistry (SSC-2016), Prague, Czech Republic, 18–23 September 2016.

***Corresponding author: Elena Asabina,** Department of Chemistry, N.I. Lobachevsky State University of Nizhni Novgorod, pr. Gagarina 23, Nizhniy Novgorod 603950, Russia, e-mail: elena.asabina@inbox.ru
Vladimir Pet'kov, Pavel Mayorov, Dmitriy Lavrenov and Igor Schelokov: Department of Chemistry, N.I. Lobachevsky State University of Nizhni Novgorod, pr. Gagarina 23, Nizhniy Novgorod 603950, Russia
Andrey Kovalsky: National University of Science and Technology, Leninskiy pr. 4, Moscow 119049, Russia

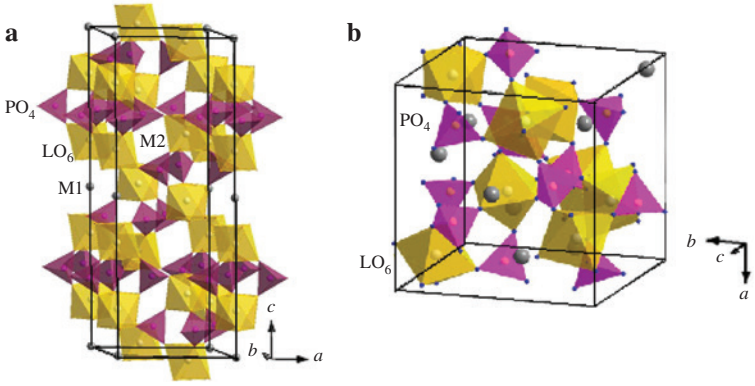

Fig. 1: Linking of $L_2(PO_4)_3$ fragments in different structural types: (a) NZP (M1 and M2–cavitiy sites); (b) scandium tungstate.

there are several (depending on the distortion of structure) cavity sites, where cations are surrounded by four nearest O atoms, in the framework cavities.

It is known [9], that $M_{0.5}Zr_2(PO_4)_3$ compounds containing large M^{2+} cations (Cd^{2+}, Ca^{2+}, Sr^{2+}, Pb^{2+}, Ba^{2+}) in the structural cavities are characterized as NZP type structure (trigonal symmetry). Substitution of large M^{2+} ions for small 3d-transition metal cations (Ni^{2+}, Cu^{2+}, Zn^{2+}, Co^{2+}, Mn^{2+}) or Mg^{2+} leads to lowering of symmetry and turning structural type into SW (monoclinic symmetry). The data related to phosphates containing metals in oxidation state +2 in the framework sites, such as $[M_{1/3}Nb_{5/3}(PO_4)_3]$ (M–Ni, Mg, Cu, Zn, Co, Mn) [10], $Na_{1+2x}[Mg_xZr_{2-x}(PO_4)_3]$ ($0 \le x \le 1$) [11], $Na_3[MZr(PO_4)_3]$ (M–Ni, Mg, Zn, Mn) [12, 13] (frameworks are shown within [brackets]) is scarce. Isomorphic substitution of Zr^{4+} for metal in oxidation state +2 in the octahedrally coordinated framework sites is possible on condition that M^{2+} ionic radii is comparable with Zr^{4+}.

In keeping with the crystal-chemical data (Table 1) [14], we made the prognosis that there is a high probability of the wide range of solid solutions to be acquired in the $M_{0.5+x}[M'_xZr_{2-x}(PO_4)_3]$ systems with framework cations M′–Ni^{2+}, Mg^{2+}, Cu^{2+}, Zn^{2+}, Co^{2+}, Mn^{2+}. We have already shown that $MgNi_{0.5}Zr_{1.5}(PO_4)_3$ has SW structure and $MNi_{0.5}Zr_{1.5}(PO_4)_3$ (M–Ca, Sr), $Ca_{0.5+x}[Zn_xE_{2-x}(PO_4)_3]$ (E–Ti, Zr; $0 \le x \le 0.5$) crystallize in NZP structure [15, 16]. Within systematic investigation of these zirconium containing systems it was of interest to study phosphates containing cations with $\Delta r/r_{min}$ varying (compared with Zr^{4+}) from 0 (Mg^{2+}) to 15 % (Mn^{2+}) in the framework sites. To compare the solid solution regions, we chose the systems with small, medium and large cations in the structural cavities.

The aim of this work was to investigate experimentally the possibility of incorporation of metals in oxidation state +2 into the framework and cavities' sites of $M_{0.5+x}M'_xZr_{2-x}(PO_4)_3$ (M–Ca, Mn, Co, Sr, Cd, Ba, Pb; M′–Mg, Mn, Co; $0 \le x \le 2.0$) phosphates. By virtue of possible practical applications of the framework substances, thermal expansion of the phosphates' representatives was examined in the temperature range from 20 to 800 °C.

Experimental

$M_{0.5+x}M'_xZr_{2-x}(PO_4)_3$ (M–Ca, Mn, Co, Sr, Cd, Ba, Pb; M′–Mg, Mn, Co; $0 \le x \le 2.0$; Table 2) phosphates were synthesized by sol-gel method. The initial reactants were the following: aqueous solutions of metal chlorides

Table 1: Geometrical parameter of ability of Zr^{4+} for M^{2+} isomorphic substitution in octahedrally coordinated sites ($r(Zr^{4+}) = 0.72$ Å).

M^{2+}	Be	Ni	Mg	Cu	Zn	Co	Mn	Cd	Ca	Sr	Pb	Ba
r (Å)	0.45	0.69	0.72	0.73	0.74	0.745	0.83	0.95	1.00	1.18	1.19	1.35
$\Delta r/r_{min}$ (%)	60	4	0	1	3	3	15	32	39	64	65	88

Table 2: Specific values of *x*, that were achieved during synthesis of $M_{0.5+x}M'_xZr_{2-x}(PO_4)_3$ compounds.

System	*x*
$Co_{0.5+x}[Mg_xZr_{2-x}(PO_4)_3]$	0, 0.25, 0.5, 0.75, 1.0, 1.1, 1.2, 1.5, 2.0
$Co_{0.5+x}[Co_xZr_{2-x}(PO_4)_3]$	0, 0.1, 0.25, 0.5, 1.0, 1.5, 2.0
$Co_{0.5}Mn_x[Co_xZr_{2-x}(PO_4)_3]$	0, 0.1, 0.25, 0.5, 0.6, 0.75, 1.0, 1.5, 2.0
$Mn_{0.5+x}[Mg_xZr_{2-x}(PO_4)_3]$	0, 0.25, 0.5, 0.75, 1.0, 1.1, 1.2, 1.5, 2.0
$Mn_{0.5+x}[Co_xZr_{2-x}(PO_4)_3]$	0, 0.1, 0.25, 0.5, 1.0, 1.5, 2.0
$Mn_{0.5+x}[Mn_xZr_{2-x}(PO_4)_3]$	0, 0.1, 0.25, 0.5, 0.6, 0.75, 1.0, 1.5, 2.0
$Cd_{0.5}Mg_x[Cd_xZr_{2-x}(PO_4)_3]$	0, 0.5, 0.6, 0.7, 0.8, 1.0, 1.5, 2.0
$Cd_{0.5+x}[M'_xZr_{2-x}(PO_4)_3]$ M′ – Co, Mn	0, 0.1, 0.2, 0.3, 0.4, 0.5, 1.0, 1.5, 2.0
$Ca_{0.5+x}[M'_xZr_{2-x}(PO_4)_3]$ M′–Mg, Co, Mn	0, 0.25, 0.5, 0.75, 1.0, 1.1, 1.2, 1.5, 2.0
$Sr_{0.5+x}[M'_xZr_{2-x}(PO_4)_3]$ M′–Mg, Co	0, 0.3, 0.4, 0.5, 0.6, 0.7, 1.0, 1.5, 2.0
$Sr_{0.5+x}[Mn_xZr_{2-x}(PO_4)_3]$	0, 0.1, 0.2, 0.3, 0.4, 0.5, 1.0, 1.5, 2.0
$Pb_{0.5+x}[Mg_xZr_{2-x}(PO_4)_3]$	0, 0.5, 0.6, 0.7, 0.8, 0.9, 1.0, 1.5, 2.0
$Pb_{0.5+x}[M'_xZr_{2-x}(PO_4)_3]$ M′–Co, Mn	0, 0.5, 0.6, 0.7, 0.8, 1.0, 1.5, 2.0
$Ba_{0.5+x}[M'_xZr_{2-x}(PO_4)_3]$ M′–Mg, Co, Mn	0, 0.1, 0.25, 0.5, 0.75, 1.0, 1.5, 2.0

or acetates, $ZrOCl_2 \cdot 8H_2O$, H_3PO_4 and $NH_4H_2PO_4$ (all reagents were chemically pure). The solutions, taken in keeping with the stoichiometry of the phosphate, were poured together under continuous stirring. Afterwards, desiccation of reaction mixture at 90 °C and heating in unconfirmed air access at 600–900 °C with a step interval of 50–100 °C for 24–48 h at each stage ensued.

The obtained samples were white or colored polycrystalline powders. Their chemical composition and homogeneity were checked with the aid of a CamScan MV-2300 microprobe with a Link INCA ENERGY 200C energy-dispersion detector. The uncertainty of the chemical composition determination was within 2–2.5 % mol.

Phase purity was confirmed with powder X-ray diffraction (XRD) at Shimadzu XRD-6000 diffractometer (CuK_α radiation). Unit cell parameters of the compounds were determined at a room temperature from the corresponding diffraction patterns indexed within 2θ range 10–60 deg. with step being 0.02 deg. and the rate of 1 deg./min. Data for the structure refinement were collected within 2θ range 10–90(110) deg. with step being 0.02 deg. and preset time in every point 12 s. Structure refinement was performed by Rietveld method [17] via Rietan-97 program [18]. X-ray patterns for thermal expansion study were obtained in the 2θ interval 10–60 deg. with step being 0.02 deg. and the rate of 1 deg./min, at the temperature range from 20 to 800 °C.

Functional composition of the samples was confirmed by IR spectroscopy on Shimadzu FTIR 8400S spectrometer within range 1400–400 cm^{-1}.

Thermal behavior of the synthesized samples was investigated by differential thermal analysis (DTA) on Labsys TG-DTA/DSC thermoanalyzer in a continuous heating regime. Experiment was undertaken in the interval 25–950 °C, with the heating and cooling rates being 10 °C/min.

Results and discussion

Synthesis

Phase formation of the complex phosphates was studied with the use of X-ray powder diffraction of the reaction mixtures from the consequent temperature stages. For example, the results of the phase analysis of the $Mn_{0.5+x}[Mn_xZr_{2-x}(PO_4)_3]$ system are shown in Fig. 2a. Solid solutions were formed in the composition array $0 \le x \le 0.25$. Phase mixtures of the boundary solid solution $Mn_{0.75}[Mn_{0.25}Zr_{1.75}(PO_4)_3]$, ZrP_2O_7, ZrO_2, $Mn_2P_2O_7$ were observed in the samples with $x > 0.25$.

Influence of temperature on the formation of solid solution is shown in Fig. 2b. The target product $Mn_{0.75}[Mn_{0.25}Zr_{1.75}(PO_4)_3]$ was formed in the sample treated at the temperatures from 600 to 750 °C. Its crystallinity built up with the increase of temperature, but at $T > 750$ °C decomposition of the phosphate started.

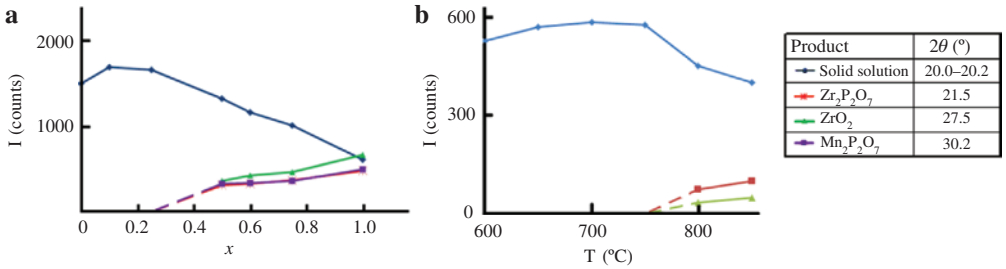

Fig. 2: Results of X-ray study of phase formation in the $Mn_{0.5+x}Mn_xZr_{2-x}(PO_4)_3$ system: (a) Intensity of the main diffraction peaks for the phases in the XRD pattern *vs.* sample composition (temperature of thermal treatment is 650 °C); (b) Intensity of the main diffraction peaks for the phases in the XRD pattern *vs.* temperature of the sample treatment (time of every isothermal stage was 24 h).

Characterization of the samples

XRD results showed, that the phosphates with the common formula $M_{0.5+x}M'_xZr_{2-x}(PO_4)_3$ (M–Mn, Co; M′–Mg, Mn, Co) crystallize in the SW structural type.

Incorporation of Mg^{2+} (close to Zr^{4+} by ionic radius) into the framework sites leaded to comparatively wide solid solutions regions in the system $Mn_{0.5+x}Mg_xZr_{2-x}(PO_4)_3$ ($0 \le x \le 1.0$). Single phase compounds were synthesized at 650–700 °C and remained intact up to 850 °C. Samples with $x > 1.0$ consisted of phosphate with $x = 1$, $Mg_3(PO_4)_2$ and $Mn_3(PO_4)_2$ (Fig. 3a).

The powder XRD data of the single-phase samples showed a similar distribution of Bragg reflections in the patterns of $Mn_{0.5+x}Mg_xZr_{2-x}(PO_4)_3$ ($0 \le x \le 1.0$) with smooth changing in their relative intensities and 2θ values across the studied compositions' range. The phosphates were indexed with space group $P2_1/n$.

The results of electron microprobe analysis confirmed the homogeneity of the samples and indicated that their compositions were close to the theoretical ones.

The IR spectra of the synthesized single-phase samples (Fig. 3b) were typical for the orthophosphates that crystallize in SW structure. Factor-group analysis predicted the maximum amount of characteristic PO_4 vibrations, being six asymmetric stretching ν_1, 12 symmetric stretching ν_2, 18 asymmetric ν_3 and 18 symmetric bending ν_4. The spectra showed less experimental number of absorption bands: the broad absorption bands at 1260–1020 cm^{-1}, ν_3; 1000–900 cm^{-1}, ν_1; 650–550 cm^{-1}, ν_4. Shift and intensity redistribution of absorption bands were observed in the spectral patterns with changing of phosphates' composition.

XRD results allowed us to calculate unit cell parameters of the obtained phosphates. Incorporation of Mn^{2+} cations in the structural cavities leaded to escalation of the cell distortion (raise of monoclinic angle β

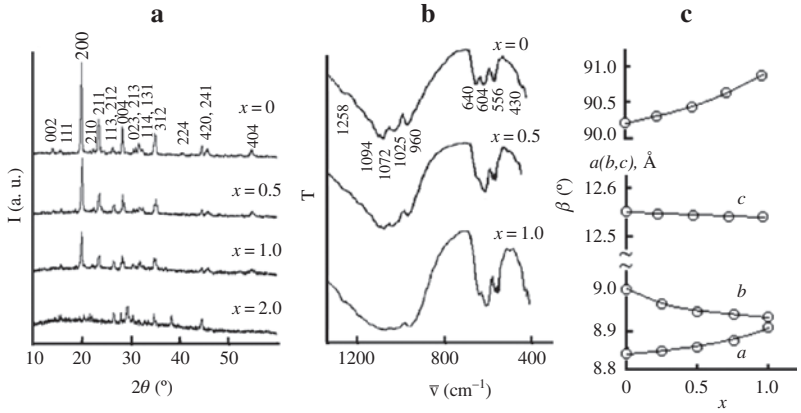

Fig. 3: Characterization of the $Mn_{0.5+x}Mg_xZr_{2-x}(PO_4)_3$ samples: (a) X-ray patterns; (b) IR spectra; (c) lattice parameters.

difference from 90°) with corresponding monotonous increase of *a* parameter, decrease of *b* and *c* parameters (Fig. 3c).

Composition (*x*) regions of SW structure for other systems containing manganese were more shrunk, than in case of $Mn_{0.5+x}Mg_xZr_{2-x}(PO_4)_3$: $0 \le x \le 0.25$ for $Mn_{0.5+x}Mn_xZr_{2-x}(PO_4)_3$, $x = 0$ for $Mn_{0.5+x}Co_xZr_{2-x}(PO_4)_3$. Single phase compounds were synthesized at 650 °C and remained stable up to 900–1000 °C. Other samples of these rows were found to be mixtures of SW structure phases with $Mn_3(PO_4)_2$ (or $Co_3(PO_4)_2$).

The results of the study of $M_{0.5+x}M'_xZr_{2-x}(PO_4)_3$ (M–Ca, Sr, Cd, Pb; M′–Mg, Mn, Co) phosphates showed formation of limited solid solutions of NZP type.

In particular, the NZP solid solutions formed in the region $0 \le x \le 1.0$ for the $Ca_{0.5+x}Co_xZr_{2-x}(PO_4)_3$ system (Fig. 4). X-ray patterns of the phosphates were indexed in the space group $R\bar{3}$. Synthesis temperature was 700–800 °C. The compounds were stable up to 850–1100 °C.

IR spectra confirmed that investigated compounds belong to the NZP orthophosphates class (Fig. 4b). It may be deduced from the factor group analysis that maximum amount of characteristic PO_4 vibrations is 6 ν_3, 6 ν_4, 4 ν_2 and 2 ν_1. The obtained spectra were presented by 4–6 ν_3 absorption bands and characteristic (typical for NZP phosphates, $R\bar{3}$ space group) triplet of ν_4 bands. Bands of ν_1 and ν_2 vibrations were observed at 645–540 cm^{-1} and ≤500 cm^{-1}, respectively.

Unit cell *a* and *c* parameters of the studied solid solutions (Fig. 4c) depend on several factors. The *a* parameter is the function of width of (Co or Zr)O_6 and PO_4 polyhedra columns, while the *c* parameter is related to structural fragments height. The difference in Co^{2+} and Zr^{4+} ionic radii is not big, so this factor had weak influence on the *a* and *c* parameters. Incorporation of Ca^{2+} ions in the structural cavities (with *x* growth) leaded to the increase of polyhedra columns height. Corresponding polyhedra deformation caused *a* parameter to decrease, in line with *x* growth (as described in [1]).

It is known [19], that polymorphic phase transitions were observed for $CaM'_{0.5}Zr_{1.5}(PO_4)_3$ (M′–Mg, Mn). These compounds crystallized in the NZP structure during synthesis at 700 °C, whereas they underwent irreversible transition into orthorhombic symmetry phase (space group *Pnma*) at higher temperatures, in which Mn^{2+} and Ca^{2+} form polyhedra with coordination number seven.

To investigate $CaCo_{0.5}Zr_{1.5}(PO_4)_3$ thermal behavior, DTA study of the sample (obtained at 700 °C) was carried out (Fig. 5a). The exothermic effect 859–876 °C was observed on the DTA curve of the phosphate. X-ray pattern of the $CaCo_{0.5}Zr_{1.5}(PO_4)_3$ sample, treated at 900 °C for 24 h (Fig. 5b), showed that the sample comprised of NZP phosphate and orthorhombic phase, similar to described in [19].

Overall, XRD and IR spectroscopy data were in a good agreement. There was resemblance among the obtained data on the structural types, unit cell parameters and IR spectra of phosphates with $x = 0$ and the literature ones [9]. The study of triple phosphates revealed the existence of solid solutions in the $M_{0.5+x}M'_xZr_{2-x}(PO_4)_3$ (M–Ca, Mn, Co, Sr, Cd, Pb; M′–Mg, Mn, Co) systems. Phosphates with M–Ba were exception to the pattern: NZP phase in these systems was obtained only for $x = 0$, compounds with $x = 0.5$ crystallized in the yavapaiite ($KFe(SO_4)_2$ [20]) structure, and there were no solid solutions observed within any significant regions.

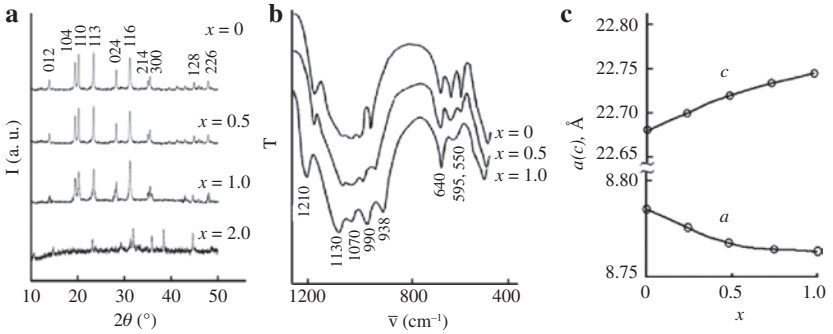

Fig. 4: Characterization of the $Ca_{0.5+x}Co_xZr_{2-x}(PO_4)_3$ samples: (a) X-ray patterns; (b) IR spectra; (c) lattice parameters.

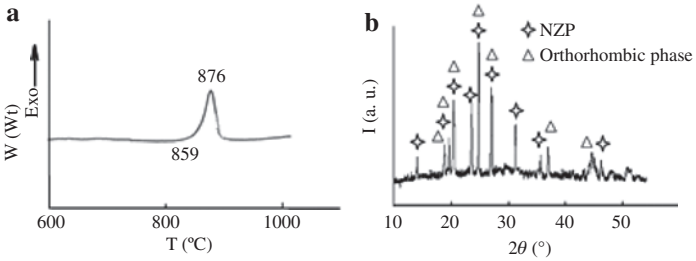

Fig. 5: $CaCo_{0.5}Zr_{1.5}(PO_4)_3$ phase transition study: (a) DSC curve; (b) X-ray pattern of the sample treated at 900 °C for 24 h.

Structural investigation

With the aim of making distribution of metals M, M′ in the crystallographic sites (framework and cavities) clear, we refined the crystal structures of triple phosphates with $x = 0.5$ of the compositions $MnMg_{0.5}Zr_{1.5}(PO_4)_3$ (SW), $CoMn_{0.5}Zr_{1.5}(PO_4)_3$ (SW) и $CaCo_{0.5}Zr_{1.5}(PO_4)_3$ (NZP) by the Rietveld method using X-ray powder diffraction data.

For the initial fractional coordinates, that are indispensable for Rietveld analysis, we used those of $Ni_{0.5}Zr_2(PO_4)_3$ (SW, space group $P2_1/n$) [21] and $Cd_{0.5}Zr_2(PO_4)_3$ (NZP, space group $R\bar{3}$) [22]. The experimental and refinement conditions, lattice parameters and *R* factors are presented in Table 3.

There are two types of octahedrally coordinated framework sites ($2\times4e$) in the SW structure. It was established, that one type of sites is filled by Zr^{4+} cations, while another one is occupied by statistically distributed Mg^{2+} (or Co^{2+}) and Zr^{4+} cations of comparable sizes. Cavity sites ($4e$) are occupied by cations of larger average sizes than those of the framework ones: Mn^{2+} in $MnMg_{0.5}Zr_{1.5}(PO_4)_3$, Mn^{2+} together with Co^{2+} in $CoMn_{0.5}Zr_{1.5}(PO_4)_3$ structure.

There are also two types of framework-forming cationic sites ($2\times6c$) in the $CaCo_{0.5}Zr_{1.5}(PO_4)_3$ (NZP) structure. These positions are occupied by Zr^{4+} and Co^{2+}/Zr^{4+} ions, correspondingly. The peculiarity of space group $R\bar{3}$ is that M1 cavities sites are divided into two types ($3a$ and $3b$, surrounded by two types of the framework octahedra), and that Ca^{2+} cations fill both types of these sites within the octahedral-tetrahedral columns. Varying occupancy of M2 sites showed that the sites remain vacant.

The observed, calculated and difference XRD patterns are shown in Fig. 6a. Obviously, the observed patterns were in a good agreement with the calculated ones. The final fractional coordinates and isotropic atomic displacement parameters are listed in Tables 4–6.

Table 3: Conditions of X-ray diffraction experiment and refinement results for $MM'_{0.5}Zr_{1.5}(PO_4)_3$ phosphates.

Compound	$Mn[Mg_{0.5}Zr_{1.5}(PO_4)_3]$	$Co_{0.5}Mn_{0.5}[Co_{0.5}Zr_{1.5}(PO_4)_3]$	$Ca[Co_{0.5}Zr_{1.5}(PO_4)_3]$
Space group	$P2_1/n$	$P2_1/n$	$R\bar{3}$
Z	4	4	6
2θ range (deg.)	10–90	10–90	10–110
Unit cell parameters			
a (Å)	8.847(3)	8.8317(14)	8.7677(3)
b (Å)	8.970(3)	8.9664(11)	–
c (Å)	12.453(4)	12.441(2)	22.715(2)
β (°)	90.47(2)	90.20(2)	–
V (Å ^{3})	988.2(5)	985.2(2)	1512.23(4)
Number of reflections	795	792	429
Variables			
Structural	76	76	26
Other	22	22	20
Reliabililty factors (%)			
R_{wp}; R_p	7.33; 5.18	2.17; 1.52	3.13; 2.19

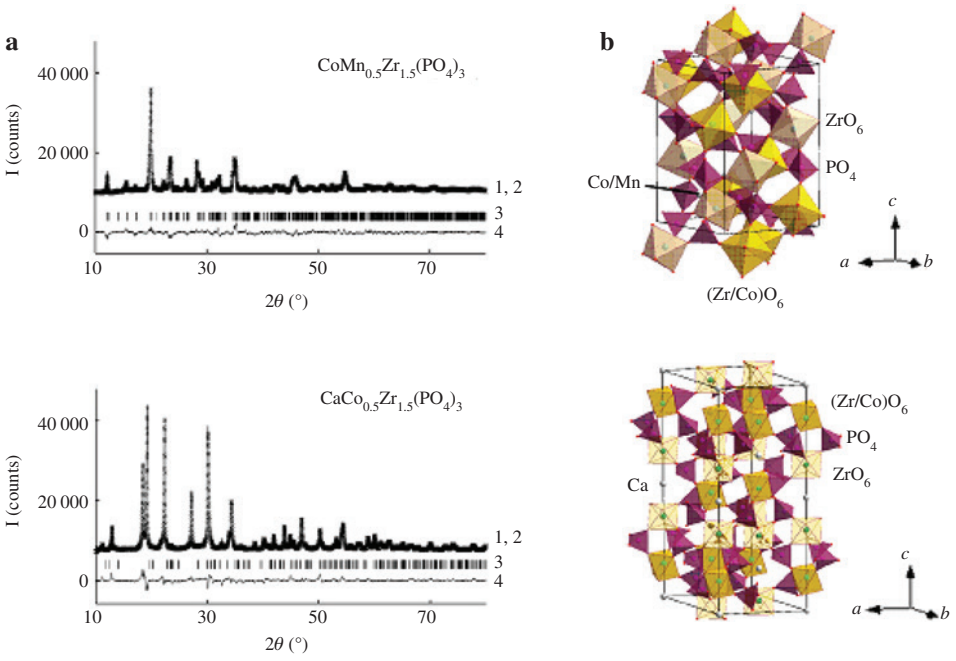

Fig. 6: Results of Rietveld structure refinement: (a) Portions of the observed (1), calculated (2), difference (3) Rietveld refinement profiles and Bragg reflections (4) for XRD patterns of the studied phosphates; (b) Fragments of their crystal structures.

Table 4: Fractional coordinates and isotropic atomic displacement parameters for $Mn[Mg_{0.5}Zr_{1.5}(PO_4)_3]$.

Atom	Site	*g*	*x*	*y*	*z*	*B* (Å²)
Mn(1)	4*e*	1	0.1694(4)	0.2023(5)	0.7147(5)	2.8(4)
Zr(1)	4*e*	1	0.1160(3)	0.0227(5)	0.2518(4)	2.4(5)
Zr(2)/Mg(2)	4*e*	1	0.3878(5)	0.0407(3)	0.7464(4)	2.2(5)
P(1)	4*e*	1	0.5054(5)	0.2548(3)	0.4630(4)	0.78(9)
P(2)	4*e*	1	0.1479(4)	0.3764(2)	0.3990(5)	1.5(5)
P(3)	4*e*	1	0.3569(4)	0.3972(4)	0.8886(3)	2.0(6)
O(1)	4*e*	1	0.585(2)	0.335(1)	0.562(1)	1.7(4)
O(2)	4*e*	1	0.572(1)	0.171(2)	0.351(2)	2.6(5)
O(3)	4*e*	1	0.424(3)	0.353(1)	0.383(2)	1.4(7)
O(4)	4*e*	1	0.431(2)	0.143(1)	0.556(1)	2.0(5)
O(5)	4*e*	1	0.175(2)	0.219(1)	0.373(2)	1.6(2)
O(6)	4*e*	1	0.036(1)	0.427(1)	0.338(2)	0.65(7)
O(7)	4*e*	1	0.164(2)	0.408(1)	0.565(1)	0.48(5)
O(8)	4*e*	1	0.225(1)	0.484(2)	0.315(2)	3.0(7)
O(9)	4*e*	1	0.332(2)	0.240(1)	0.829(1)	2.9(7)
O(10)	4*e*	1	0.364(1)	0.396(2)	0.051(2)	1.6(7)
O(11)	4*e*	1	0.464(2)	0.445(1)	0.817(3)	2.9(8)
O(12)	4*e*	1	0.271(1)	0.513(1)	0.833(2)	2.9(6)

In the chosen models all *B* parameters were positive and reasonable. The bond lengths in the cavities' and framework-forming polyhedra in the studied structures (Table 7) were in agreement with the corresponding data for other NZP and SW phosphates [14, 21–23]. The corresponding average distances were close to each other for the one type of phosphates (SW), in spite of large scale dispersions of interatomic distances within the polyhedra. Larger NZP cavities sizes compared with the SW ones may be clearly observed.

The fragments of the studied phosphates structures are shown in Fig. 6b. The framework fragments of three corner-sharing PO_4-tetrahedra and two types of octahedra were in the basis of all presented structures.

Table 5: Fractional coordinates and isotropic atomic displacement parameters for $Co_{0.5}Mn_{0.5}[Co_{0.5}Zr_{1.5}(PO_4)_3]$.

Atom	Site	*g*	*x*	*y*	*z*	*B* (Å²)
Mn(1)/Co(1)	4*e*	1	0.7096(6)	0.2206(7)	0.1701(3)	2.7(8)
Zr(1)	4*e*	1	0.7459(19)	0.0275(9)	0.3868(7)	1.9(7)
Zr(2)/Co(2)	4*e*	1	0.253(2)	0.0317(11)	0.1222(9)	1.2(5)
P(1)	4*e*	1	0.4601(3)	0.2555(8)	0.5029(3)	2.9(2)
P(2)	4*e*	1	0.3971(5)	0.3795(6)	0.1431(7)	2.5(5)
P(3)	4*e*	1	0.8872(4)	0.3964(7)	0.3559(8)	2.0(6)
O(1)	4*e*	1	0.5709(8)	0.3312(8)	0.5764(7)	2.9(9)
O(2)	4*e*	1	0.3538(3)	0.1723(3)	0.5687(5)	2.4(4)
O(3)	4*e*	1	0.3822(8)	0.3570(7)	0.4258(6)	1.9(8)
O(4)	4*e*	1	0.5592(4)	0.1480(4)	0.4344(3)	2.2(2)
O(5)	4*e*	1	0.3758(2)	0.2094(8)	0.1684(2)	1.0(4)
O(6)	4*e*	1	0.3463(2)	0.4246(6)	0.0320(5)	1.6(7)
O(7)	4*e*	1	0.5598(7)	0.4034(5)	0.1628(5)	2.3(2)
O(8)	4*e*	1	0.3157(3)	0.4829(5)	0.2273(6)	1.8(4)
O(9)	4*e*	1	0.8282(4)	0.2418(2)	0.3359(6)	1.4(5)
O(10)	4*e*	1	0.0516(5)	0.3909(2)	0.3685(4)	1.8(4)
O(11)	4*e*	1	0.8105(7)	0.4482(5)	0.4610(4)	1.9(7)
O(12)	4*e*	1	0.8336(2)	0.5162(4)	0.2648(2)	1.2(4)

Table 6: Fractional coordinates and isotropic atomic displacement parameters for $Ca[Co_{0.5}Zr_{1.5}(PO_4)_3]$.

Atom	Site	*g*	*x*	*y*	*z*	*B* (Å²)
Ca(1)	3*a*	1	0	0	0	2.1(4)
Ca(2)	3*b*	1	0	0	0.5	3.4(2)
Zr(1)/Co(1)	6*c*	1	0	0	0.1496(5)	0.49(7)
Zr(2)	6*c*	1	0	0	0.6412(4)	0.96(3)
P(1)	18*f*	1	0.2853(2)	0.0012(4)	0.2503(3)	0.31(2)
O(1)	18*f*	1	0.1852(2)	−0.0107(7)	0.1891(9)	0.53(4)
O(2)	18*f*	1	0.0647(3)	0.8456(3)	0.6941(4)	0.97(5)
O(3)	18*f*	1	0.1838(2)	0.1870(6)	0.0890(2)	0.91(6)
O(4)	18*f*	1	0.2103(3)	0.0655(5)	0.5970(5)	0.97(9)

These fragments formed columns parallel to one another in NZP compound $CaCo_{0.5}Zr_{1.5}(PO_4)_3$ and columns oriented in two alternating directions in SW phosphates $MnMg_{0.5}Zr_{1.5}(PO_4)_3$ and $CoMn_{0.5}Zr_{1.5}(PO_4)_3$.

Different packing of the same fragments leaded to the variation in size, form, location and amount of framework cavities. In our case, Mn^{2+} ($r = 0.66$ Å) and Co^{2+} ($r = 0.58$ Å) occupied relatively small tetrahedrally coordinated cavities of SW structures, while Ca^{2+} ($r = 1.00$ Å) ions occupied comparatively large cavities of NZP structure. Thus, the structural framework adapted to the size of located M^{2+} cations in its cavities.

Unusual cations distribution was found by ourselves [24] for the $CdMg_{0.5}Zr_{1.5}(PO_4)_3$ structure earlier. The results of Rietveld refinement of cations' occupations within structural sites indicated that one type of the framework sites was filled with Zr^{4+} ions, whereas Cd^{2+} ($r = 0.95$ Å) and Zr^{4+} ($r = 0.72$ Å) were statistically distributed in another type. Interatomic distances showed that combined framework octahedra were far more distorted [$(d_{min}-d_{max}) = 1.862$–$2.237$ Å] than Zr-based ones (2.006–2.187 Å). Cavities within the polyhedra columns were occupied by alternating Cd^{2+} and Mg^{2+} ions. Isomorphic substitution of Zr^{4+} by Cd^{2+} (not Mg^{2+}, which is close to Zr^{4+} by ionic radius $r = 0.72$ Å) may probably be explained by the proximity of Zr ($4d^25s^2$) electronic structure to Cd ($4d^{10}5s^2$) one. In this case it exerted greater effect than size factor.

Basing on the results of this study, we made comparison between the concentration regions of NZP and SW-type phases existence in the $M_{0.5+x}M'_xZr_{2-x}(PO_4)_3$ (M–Ca, Mn, Co, Sr, Cd, Ba, Pb; M′–Mg, Mn, Co; $0 \le x \le 2.0$) systems (Table 8).

Table 7: Bond lengths in structure-forming polyhedra of the studied phosphates.

Polyhedron	Interval of bond lengths (d_{min}–d_{max}), Å	Average bond length <*d*>, Å
$Mn[Mg_{0.5}Zr_{1.5}(PO_4)_3]$		
MnO_6	1.902–2.281	2.13
ZrO_6	1.994–2.186	2.09
$(Zr/Mg)O_6$	1.996–2.153	2.08
PO_4	1.499–1.598	1.53
	1.470–1.558	1.52
	1.439–1.567	1.52
$Co_{0.5}Mn_{0.5}[Co_{0.5}Zr_{1.5}(PO_4)_3]$		
$(Mn/Co)O_4$	2.036–2.318	2.13
ZrO_6	2.013–2.151	2.08
$(Zr/Co)O_6$	2.010–2.141	2.07
PO_4	1.454–1.558	1.50
	1.473–1.575	1.53
	1.461–1.631	1.53
$Ca[Co_{0.5}Zr_{1.5}(PO_4)_3]$		
CaO_6	2.594	2.59
	2.743	2.74
ZrO_6	1.918–2.090	2.00
$(Zr/Co)O_6$	1.898–2.130	2.01
PO_4	1.560–1.621	1.60

Table 8: Concentration limits of $M_{0.5+x}M'_xZr_{2-x}(PO_4)_3$ solid solutions existence.

System	Limits *x*	Structure type
$Co_{0.5+x}[Mg_xZr_{2-x}(PO_4)_3]$	$0 \le x \le 1.0$	SW
$Co_{0.5+x}[Co_xZr_{2-x}(PO_4)_3]$	$x = 0$	SW
$Co_{0.5}Mn_x[Co_xZr_{2-x}(PO_4)_3]$	$0 \le x \le 0.5$	SW
$Mn_{0.5+x}[Mg_xZr_{2-x}(PO_4)_3]$	$0 \le x \le 1.0$	SW
$Mn_{0.5+x}[Co_xZr_{2-x}(PO_4)_3]$	$x = 0$	SW
$Mn_{0.5+x}[Mn_xZr_{2-x}(PO_4)_3]$	$0 \le x \le 0.25$	SW
$Cd_{0.5}Mg_x[Cd_xZr_{2-x}(PO_4)_3]$	$0 \le x \le 0.6$	NZP
$Cd_{0.5+x}[M'_xZr_{2-x}(PO_4)_3]$ M′ – Co, Mn	$0 \le x \le 0.3$	NZP
$Ca_{0.5+x}[M'_xZr_{2-x}(PO_4)_3]$ M′–Mg, Co, Mn	$0 \le x \le 1.0$	NZP
$Sr_{0.5+x}[M'_xZr_{2-x}(PO_4)_3]$ M′–Mg, Co	$0 \le x \le 0.5$	NZP
$Sr_{0.5+x}[Mn_xZr_{2-x}(PO_4)_3]$	$0 \le x \le 0.3$	NZP
$Pb_{0.5+x}[Mg_xZr_{2-x}(PO_4)_3]$	$0 \le x \le 0.7$	NZP
$Pb_{0.5+x}[M'_xZr_{2-x}(PO_4)_3]$ M′–Co, Mn	$0 \le x \le 0.6$	NZP
$Ba_{0.5+x}[M'_xZr_{2-x}(PO_4)_3]$ M′–Mg, Co, Mn	$x = 0$	NZP
	$x = 0.5$	yavapaiite

On the whole, phase formation of the compounds was influenced by cations sizes ratio and isomorphic substitution of Zr^{4+} for M^{2+}. Optimal conditions for the formation of SW structure were implemented in case, when the average ionic radius of cavities cations is comparable with those of framework-forming cations. If the size discrepancy is more significant, NZP structure formed.

Ability of the M^{2+} cation to the isomorphic substitution of Zr^{4+} is clearly observed in the SW systems. The widest solid solutions regions were formed in the Mg-containing phosphates rows that may be explained by the closeness of Mg^{2+} and Zr^{4+} ionic radii.

The widest solid solution limits in the NZP systems were obtained for phosphates, containing Ca^{2+} ions, which ionic radius is supposed to be optimal for NZP interstitial sites.

Thermal expansion

The obtained solid solutions limits may be useful for crystal chemical design of materials with smoothly changing properties. As possible fields of application of the framework phosphates imply using them in the conditions of high temperatures or thermal shocks, their thermal expansion is needed to be known.

Thermal expansion of ceramic characterizes structure deformation caused by growth of temperature increase. That depends on many factors, in particular on the occupation of structural sites by cations. NZP phosphates $M_{0.5}Zr_2(PO_4)_3$ ($x=0$) with half-occupied cavities are well-known in literature, and their thermal expansion was widely studied [1]. The majority of studied phosphates are characterized by low average expansion coefficients, albeit high expansion anisotropy.

In the present investigation we studied thermal expansion of the representatives of triple NZP phosphates with occupied cavities ($x=0.5$): $Cd_{0.5}Mg_{0.5}[Cd_{0.5}Zr_{1.5}(PO_4)_3]$, $Ca[Mn_{0.5}Zr_{1.5}(PO_4)_3]$, $Pb[Mg_{0.5}Zr_{1.5}(PO_4)_3]$. The phosphates were investigated by X-ray powder diffraction in the temperature interval 20–800 °C (Fig. 7).

The compounds showed a certain pattern and also belonged to materials with low average thermal expansion (Table 9). The average expansion coefficient became lower with the increase of average radius of the cation that occupies the cavities of the structure. The least average thermal expansion coefficient and least expansion anisotropy were observed for the $Pb[Mg_{0.5}Zr_{1.5}(PO_4)_3]$ phosphate that may be connected with high deformation of its structure at room temperature because of relatively large Pb^{2+} ions in its cavities. So structure deformations are depressed with the temperature increase. The same tendency was observed earlier for other NZP compounds with occupied cavities (for example, alkali metals containing $AZr_2(PO_4)_3$ (A–Na, K Rb, Cs) [1] and seems to be a general trend for this class of substances.

On the whole, low thermal expansion of the NZP compounds combined with their high temperature stability allows us to propose NZP ceramics as perspective thermal-shock resistant materials and hope to succeed in extending their application scope.

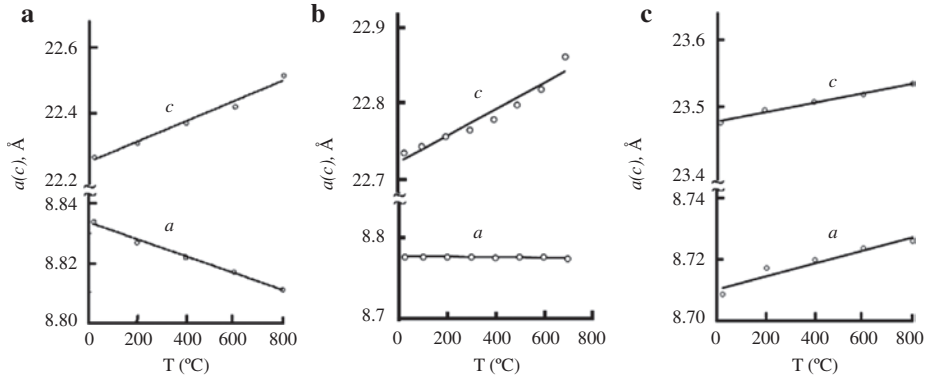

Fig. 7: Temperature dependences of lattice parameters of the phosphates: (a) $Cd_{0.5}Mg_{0.5}[Cd_{0.5}Zr_{1.5}(PO_4)_3]$; (b) $Ca[Mn_{0.5}Zr_{1.5}(PO_4)_3]$; (c) $Pb[Mg_{0.5}Zr_{1.5}(PO_4)_3]$.

Table 9: Thermal expansion of the triple NZP phosphates with $x=0.5$.

Phosphate	$r_{cavity\ ion}/r_{framework\ ion}$	Linear coefficients of thermal expansion, $\alpha\ 10^6\ °C^{-1}$			Anisotropy $\lvert\alpha_a-\alpha_c\rvert \cdot 10^6\ °C^{-1}$
		α_a	α_c	α_{av}	
$Cd_{0.5}Mg_{0.5}[Cd_{0.5}Zr_{1.5}(PO_4)_3]$	1.1	−3.2	1.4	2.5	4.6
$Ca[Mn_{0.5}Zr_{1.5}(PO_4)_3]$	1.3	−0.3	7.7	2.3	8.0
$Pb[Mg_{0.5}Zr_{1.5}(PO_4)_3]$	1.6	1.9	2.6	2.2	0.7

Conclusions

Overall, isomorphism regularities in the SW and NZP-type phosphate systems containing cations in oxidation state +2 have been studied.

The structural data illustrating the preferable distribution of M^{2+} (M'^{2+}) cations in crystallographic framework and cavities sites expand the whole scope of isomorphic ability of the structures based on $\{[L_2(PO_4)_3]^{p-}\}_{3\infty}$ frameworks.

The present data demonstrate that thermal expansion of NZP materials can be adjusted to suit materials' need by proper ionic substitutions and opting for certain techniques of materials' production. Some NZP materials have very low thermal expansion and expansion anisotropy and exhibit high thermal shock resistance.

Acknowledgments: This work was supported by the Russian Foundation for Basic Research, Projects Nos.15-03-00716, 16-33-00888.

References

[1] V. I. Pet'kov, A. I. Orlova. *Inorg. Mater.* **39**, 1013 (2003).
[2] Low Thermal Expansion Ceramics Co. (LoTEC) Inc. *Amer. Ceram. Soc. Bull.* **76**, 71 (1997).
[3] J. B. Goodenough, H. Y.-P. Hong, J. A. Kafalas. *Mater. Res. Bull.* **11**, 203 (1976).
[4] V. Pet'kov, E. Asabina, V. Loshkarev, M. Sukhanov. *J. Nucl. Mater.* **471**, 122 (2016).
[5] E. A. Asabina, N. V. Orekhova, M. M. Ermilova, V. I. Pet'kov, I. O. Glukhova, N. A. Zhilyaeva, A. B. Yaroslavtsev. *Inorg. Mater.* **51**, 793 (2015).
[6] V. I. Pet'kov, G. I. Dorokhova, A. I. Orlova. *Crystallogr. Rep.* **46**, 69 (2001).
[7] M. E. Brownfield, E. E. Foord, S. J. Sutley, T. Botinelly. Am. Mineral. **78**, 653 (1993).
[8] V. A. Efremov, B. I. Lazoryak, V. K. Trunov. *Kristallographiya* **26**, 72 (1981) (In Russian).
[9] V. I. Pet'kov, V. S. Kurazhkovskaya, A. I. Orlova, M. L. Spiridonova. *Crystallogr. Rep.* **47**, 736 (2002).
[10] V. I. Pet'kov, A. I. Orlova, M. V. Sukhanov, M. V. Zharinova, V. S. Kurazhkovskaya. *J. Mater. Sci. Lett.* **21**, 513 (2002).
[11] C. Jäger, S. Barth, A. Feltz, G. Scheler. *Physica Status Solidi.* **102**, 791 (1987).
[12] M. Chakir, A. El Jazouli, D. de Waal. *Solid State Chem.* **179**, 1883 (2006).
[13] A. Feltz, S. Barth, M. Andratschke, Ch. Jäger. *J. Less-Common Metals*. **137**, 43 (1988).
[14] R. D. Shannon. *Acta Cryst.* **A32**, 751 (1976).
[15] M. V. Sukhanov, I. A. Schelokov, V. I. Pet'kov, E. R. Gobechiya, Yu. K. Kabalov, A. V. Markin, N. N. Smirnova. *Eur. Chem.-Tech. J.* **12**, 241 (2010).
[16] V. I. Pet'kov, E. V. Zhilkin, E. A. Asabina, E. Yu. Borovikova. *Rus. J. Inorg. Chem.* **59**, 1087 (2014).
[17] H. M. Rietveld. *Acta Crystallogr.* **22**, 151 (1967).
[18] Y. I. Kim, F. Izumi. *J. Ceram. Soc. Jpn.* **102**, 401 (1994).
[19] M. Orlova, L. Perfler, M. Tribus, P. Salnikov, B. Glorieux, A. Orlova. *J. Solid State Chem.* **235**, 36 (2016).
[20] E. J. Graeber, A. Rosenzweig. *Am. Mineral.* **56**, 1917 (1971).
[21] A. Jouanneaux, A. Verbaere, Y. Piffard, A. N. Fitch, M. Kinoshita. *Eur. J. Solid State Inorg. Chem.* **28**, 683 (1991).
[22] R. Brochu, M. El-Yacoubi, M. Louer, A. Serghini. M. Alami. D. Louër. *Mater. Res. Bull.* **32**, 15 (1997).
[23] S. Senbhagaraman, T. N. Guru Row, A. M. Umarji. *J. Mater. Chem.* **3**, 309 (1993).
[24] E. A. Asabina, V. E. Shatunov, V. I. Pet'kov, E. Yu. Borovikova, A. M. Kovalskii. *Rus. J. Inorg. Chem.* **61**, 811 (2016).